






RESEARCH ARTICLE | MARCH 01 2023

Resonance control method to suppress the self and mutual inductances of a 3-phase magnetic navigation system for fast drilling motion of micro helical robots

Special Collection: [67th Annual Conference on Magnetism and Magnetic Materials](#)

J. Kwon ; J. Sa ; D. Lee ; G. Jang  



AIP Advances 13, 035101 (2023)
<https://doi.org/10.1063/9.0000385>



CrossMark

AIP Advances

Why Publish With Us?



25 DAYS
average time
to 1st decision



740+ DOWNLOADS
average per article



INCLUSIVE
scope

Learn More



Resonance control method to suppress the self and mutual inductances of a 3-phase magnetic navigation system for fast drilling motion of micro helical robots

Cite as: AIP Advances 13, 035101 (2023); doi: 10.1063/9.0000385

Submitted: 28 September 2022 • Accepted: 15 February 2023 •

Published Online: 1 March 2023



View Online



Export Citation



CrossMark

J. Kwon,  J. Sa,  D. Lee,  and G. Jang^{a)} 

AFFILIATIONS

PREM, Department of Mechanical Engineering, Hanyang University, Seoul 04763, South Korea

Note: This paper was presented at the 67th Annual Conference on Magnetism and Magnetic Materials.

^{a)} Author to whom correspondence should be addressed: ghjang@hanyang.ac.kr

ABSTRACT

We developed a resonance control method to generate a high-speed rotating magnetic field in a three-phase magnetic navigation system composed of three electromagnets. The proposed resonance control method calculates the amplitudes and phases of voltages, while the capacitances suppressing the self and mutual inductances of the electromagnets to keep the currents and the magnitude of the rotating magnetic field constant, even if the frequency of the rotating magnetic field increases. Finally, we prototyped the three-phase magnetic navigation system and the variable capacitor module to validate the effectiveness of the proposed resonance control method experimentally.

© 2023 Author(s). All article content, except where otherwise noted, is licensed under a Creative Commons Attribution (CC BY) license (<http://creativecommons.org/licenses/by/4.0/>). <https://doi.org/10.1063/9.0000385>

I. INTRODUCTION

Many researchers have investigated micro helical robots actuated by an external magnetic field for possible applications to treat occlusive vascular disease. It requires a high-speed rotating magnetic field (RMF) that generates fast drilling motion of the micro helical robot to tunnel through clogged lesions in blood vessels.¹⁻³ The RMF is generated by the magnetic navigation systems (MNSs) composed of multiple coils or electromagnets. However, as the frequency of the RMF increases, the impedance from the inductance of the coils consequently decreases the currents and the magnetic field density. To overcome this problem, prior researchers utilized the resonance effect by including additional capacitors to their MNS to suppress the self-inductances. Nam *et al.* suppressed the self-inductance effect by connecting the capacitors to the coils.² Further, Nguyen *et al.* proposed a two-stage control circuit based on the resonance effect with the current amplification stages.³

The MNS composed of multiple electromagnets with magnetic cores and coils can generate a larger magnetic field than the MNS with coils only. Nam *et al.* developed the closed-loop MNS

utilizing the closed magnetic circuit to maximize the magnetic flux density in the large workspace.⁴ However, the MNS with multiple electromagnets has significant mutual inductance due to the magnetic flux linkages between electromagnets. Further, any resonance method suppressing the self and mutual inductances has not been reported.

In this paper, we propose a resonance control method to suppress both the self and mutual inductances of the three-phase MNS with three electromagnets. We developed a mathematical method to determine the amplitudes and phases of voltages and the capacitances to generate the resonance. Finally, we prototyped the three-phase MNS and the variable capacitor module to verify the effectiveness of the proposed resonance control method.

II. DEVELOPMENT OF THE RESONANCE CONTROL METHOD

When the magnitude of the current flowing in each coil of the MNS composed of electromagnets is in the linear relationship with the magnetic field, the magnetic flux density B generated by the MNS

can be superposed with the magnetic flux density generated by each electromagnet in Eq. (1).

$$\mathbf{B} = \{\mathbf{K}\} \cdot \mathbf{I} \tag{1}$$

Here, $\{\mathbf{K}\}$ is the actuation matrix and each column represents the magnetic flux density when a unit current is applied to the corresponding coil. Considering a three-phase MNS on a plane composed of three electromagnets, the size of the actuation matrix is 2×3 . The three-phase current $\mathbf{I} = [I_1 \ I_2 \ I_3]^T$ required to generate an RMF with an angular frequency ω and a magnetic flux density B_0 satisfies Eq. (2) as follows:

$$\{\mathbf{K}\} \cdot \mathbf{I} = \mathbf{B} = \begin{bmatrix} B_0 \cos(\omega t) \\ B_0 \sin(\omega t) \end{bmatrix} \tag{2}$$

Equation (2) can be rewritten into Eq. (3) as follows:

$$\begin{bmatrix} k_{11} & k_{12} & k_{13} \\ k_{21} & k_{22} & k_{23} \end{bmatrix} \begin{bmatrix} |I_1| \cos(\omega t + \varphi_1) \\ |I_2| \cos(\omega t + \varphi_2) \\ |I_3| \cos(\omega t + \varphi_3) \end{bmatrix} = \begin{bmatrix} B_0 \cos(\omega t) \\ B_0 \sin(\omega t) \end{bmatrix} \tag{3}$$

where the magnitude and phase of each three-phase current are $|I_n|$ and φ_n , respectively. Equation (3) shows the relationship between the three-phase current and the RMF, and the magnitudes and phases of each current for generating the RMF can be calculated from Eq. (3).

As shown in Fig. 1, there are significant mutual inductances between adjacent electromagnets in three-phase MNS due to the magnetic flux linkages through the magnetic cores of the MNS. The voltage-current relationship of the three-phase MNS with capacitors connected to each coil can be expressed as shown in Eq. (4).

$$\begin{bmatrix} R_1 + j\left(\omega L_1 - \frac{1}{\omega C_1}\right) & j\omega M_{12} & j\omega M_{13} \\ j\omega M_{21} & R_2 + j\left(\omega L_2 - \frac{1}{\omega C_2}\right) & j\omega M_{23} \\ j\omega M_{31} & j\omega M_{32} & R_3 + j\left(\omega L_3 - \frac{1}{\omega C_3}\right) \end{bmatrix} \begin{bmatrix} |I_1| e^{j\varphi_1} \\ |I_2| e^{j\varphi_2} \\ |I_3| e^{j\varphi_3} \end{bmatrix} = \begin{bmatrix} |V_1| e^{j\psi_1} \\ |V_2| e^{j\psi_2} \\ |V_3| e^{j\psi_3} \end{bmatrix} \tag{4}$$

Here, R_k , L_k , C_k , φ_k , and ψ_k are the resistance, self-inductance, capacitance, phase of current, and phase of the voltage of the k th coil, respectively, and M_{kn} is the mutual inductance between the k th and the n th coil. After separating the real and the imaginary parts of the k th row of Eq. (4), Eq. (4) can be expressed as Eq. (5).

$$\left(R_k |I_k| - \omega \sum_{n \neq k}^3 M_{kn} |I_n| \sin(\varphi_n - \varphi_k) \right) + j \left(\omega L_k |I_k| - \frac{1}{\omega C_k} + \omega \sum_{n \neq k}^3 M_{kn} |I_n| \cos(\varphi_n - \varphi_k) \right) = |V_k| e^{j(\psi_k - \varphi_k)}, \quad (k = 1, 2, 3) \tag{5}$$

To remove all components except the pure resistance term ($R_k |I_k|$) from the real part of Eq. (5), Eq. (6) must be satisfied.

$$\begin{bmatrix} 0 & M_{12} \sin(\varphi_2 - \varphi_1) & M_{13} \sin(\varphi_3 - \varphi_1) \\ M_{21} \sin(\varphi_1 - \varphi_2) & 0 & M_{23} \sin(\varphi_3 - \varphi_2) \\ M_{31} \sin(\varphi_1 - \varphi_3) & M_{32} \sin(\varphi_2 - \varphi_3) & 0 \end{bmatrix} \begin{bmatrix} |I_1| \\ |I_2| \\ |I_3| \end{bmatrix} = \{\tilde{\mathbf{M}}\} \begin{bmatrix} |I_1| \\ |I_2| \\ |I_3| \end{bmatrix} = \begin{bmatrix} 0 \\ 0 \\ 0 \end{bmatrix} \tag{6}$$

Here, $\{\tilde{\mathbf{M}}\}$ is a skew-symmetric matrix satisfying $\{\tilde{\mathbf{M}}\}^T = -\{\tilde{\mathbf{M}}\}$ and the rank of $\{\tilde{\mathbf{M}}\}$ is 2.

On the other hand, Eq. (3) to obtain the current solution can be rewritten as Eq. (7) below.

$$\{\mathbf{K}'\} \mathbf{I} = \begin{bmatrix} k_{11} & k_{12} \\ k_{21} & k_{22} \end{bmatrix} \begin{bmatrix} |I_1| \cos(\omega t + \varphi_1) \\ |I_2| \cos(\omega t + \varphi_2) \end{bmatrix} = \begin{bmatrix} B_0 \cos(\omega t) - k_{13} |I_3| \cos(\omega t + \varphi_3) \\ B_0 \sin(\omega t) - k_{23} |I_3| \cos(\omega t + \varphi_3) \end{bmatrix} \tag{7}$$

Here, $\{\mathbf{K}'\}$ is a matrix that takes only the first and second columns of $\{\mathbf{K}\}$. In addition, by multiplying both sides of Eq. (7) by $\{\mathbf{K}'\}^{-1}$, we can show that $|I_1|$, $|I_2|$, φ_1 , and φ_2 are only functions of $|I_3|$ and φ_3 .

From this, Eq. (6) can be transformed into the following nonlinear system (8).

$$\begin{cases} f_1(|I_3|, \varphi_3) = 0 \\ f_2(|I_3|, \varphi_3) = 0 \end{cases} \tag{8}$$

$|I_3|$ and φ_3 can be determined by solving Eq. (8) from the numerical method. After substituting $|I_3|$ and φ_3 into (7), we can determine $|I_1|$, $|I_2|$, φ_1 , and φ_2 .

After setting the imaginary part of Eq. (5) to be zero to express a resonance, the appropriate values of the capacitances C_k can be determined as follows.

$$C_k = \frac{|I_k|}{\omega^2} \cdot \left(\sum_{n=1}^3 M_{kn} |I_n| \cos(\varphi_n - \varphi_k) \right)^{-1}, \quad (k = 1, 2, 3) \tag{9}$$

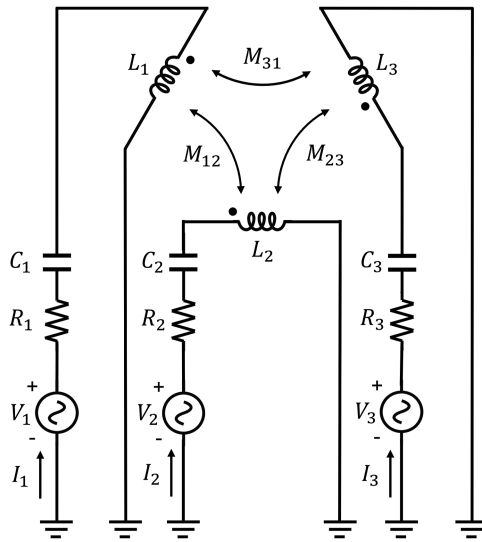


FIG. 1. The circuit diagram of the three-phase MNS.

Finally, after applying the capacitances of Eq. (9) to (5), the voltage-current relationship of each phase in Eq. (5) can be expressed as follows.

$$R_k |I_k| = |V_k| e^{j(\psi_k - \varphi_k)} = |V_k|, \quad (k = 1, 2, 3) \quad (10)$$

By substituting the current solution determined from Eq. (8) into Eqs. (9) and (10), we can determine the magnitude, phase of the applied voltage, and the required capacitances of each phase to express resonance.

As a result, the current and voltage solutions obtained through the proposed resonance control method eliminate all the imaginary parts and the real parts, except the resistance of the impedance as shown in Eq. (10). That is the input voltages to generate the RMF are independent of rotating frequency of the RMF. It also shows that the proposed method can keep the current and RMF constant even though the frequency of the RMF increases once the currents and capacitances are satisfied with Eqs. (8) and (9).

TABLE I. Major specifications of the developed three-phase MNS.

Coil number	Coil 1	Coil 2	Coil 3
Turns	105	105	210
Wire diameter (mm)	1.0	1.0	1.0
Workspace	Sphere (radius: 30 mm)		

TABLE II. Measured magnetic flux density per unit current of the developed three-phase MNS.

	Magnetic flux density per unit current (mT/A)		
	x-axis	y-axis	z-axis
Coil 1	-1.2031	1.0392	0.0178
Coil 2	1.2314	1.0434	-0.0238
Coil 3	-0.0753	-1.8185	-0.0135

TABLE III. Measured resistance and inductance of the developed three-phase MNS.

	Resistance	Inductance (mH)		
	[Ω]	Coil 1	Coil 2	Coil 3
Coil 1	14.6	2.9413	-0.7505	-0.0124
Coil 2	14.6	-0.7505	3.0255	-0.0116
Coil 3	14.8	-0.0124	-0.0116	7.5298

TABLE IV. Calculated voltage of each coil to generate the RMF of 10 mT.

	Calculated voltage		
	Coil 1	Coil 2	Coil 3
Amplitude (V)	58.1	62.3	81.0
Phase (deg)	0	178.8	265.3

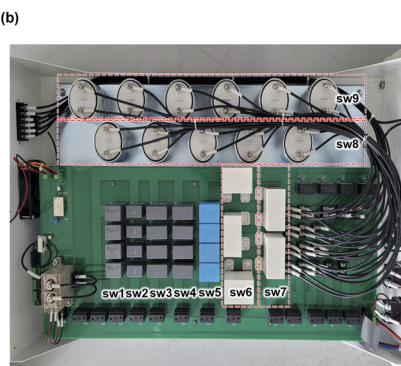
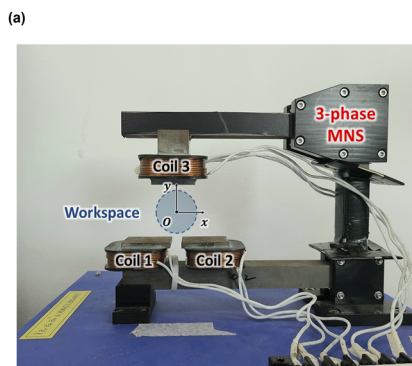


FIG. 2. (a) The three-phase MNS. (b) The variable capacitor module.

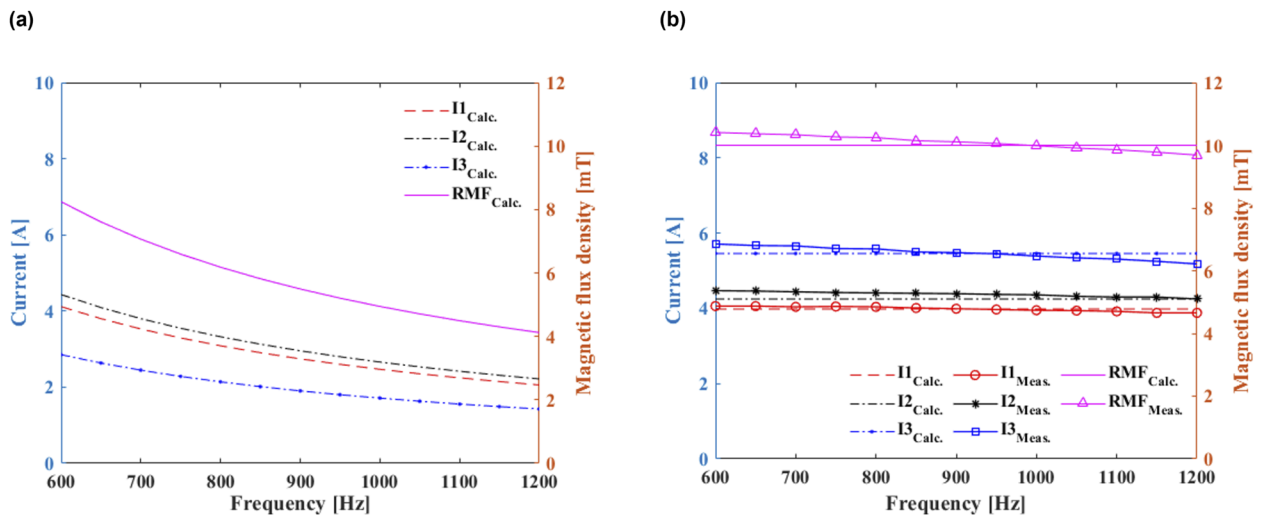


FIG. 3. (a) Decreased three-phase current and RMF due to the inductance effect. (b) Calculated and measured three-phase current and RMF with the application of the proposed method.

III. RESULTS AND DISCUSSION

To experimentally verify the effectiveness of the proposed resonance control method, we prototyped the three-phase MNS and the variable capacitor module as shown in Fig. 2. The major specifications of the MNS are presented in Table I. The three-phase MNS is connected in series with a variable capacitor module, resistors, and power supplies as shown in the circuit diagram of Fig. 1. Table II shows the measured magnetic flux densities per unit current along x , y , and z directions. We determined $\{K\}$ by choosing x and y components because the magnetic flux densities along the z -axis were less than 2% of those in the other axes as shown in Table II. Table III shows the measured resistance and inductance of the developed three-phase MNS. In addition, the capacitance can be adjusted up to $19.5 \mu\text{F}$ with a resolution of $0.055 \mu\text{F}$ using nine switches in the variable capacitor module. Next, we calculated the amplitudes and phases of the voltages and the capacitances required for resonance from the proposed method. The calculated capacitance values of each coil are 18.8 , 18.88 , and $9.34 \mu\text{F}$ at the resonance frequency of 600 Hz , and 3.01 , 3.02 , and $1.5 \mu\text{F}$ at the resonance frequency of 1200 Hz , respectively. Table IV shows the calculated amplitude and phase of the input voltages to generate an RMF with a magnetic flux density of 10 mT . Finally, we experimentally verified that the proposed resonance control method can maintain output currents and the magnitude of RMF constant even when the rotating frequency of RMF increases. In the experiment, the measured trajectory of RMF generated by the three-phase current is of circular or elliptical shape. We defined the magnitude of the RMF as a radius of a circle with a same area of the RMF trajectory. Figure 3(a) shows the decreased three-phase current and the magnitude of the RMF when the voltage solution shown in Table IV was applied. Without any resonance control method, the current and magnetic flux density decreased due to the inductance effect. We suppressed the inductance effect including mutual inductance from the proposed method. Figure 3(b) shows the calculated and measured three-phase

currents and magnitude of the RMF with the application of the proposed method to generate a magnetic flux density of 10 mT from 600 to 1200 Hz . In Fig. 3(b), the calculated current and the magnitude of RMF match well with the measured ones within 5% discrepancies. It shows that the proposed resonance control method keeps the current and the RMF constant as the rotating frequency increases.

IV. CONCLUSION

We proposed a resonance control method to suppress both the self and mutual inductances of the three-phase MNS. By separating the voltage equation of the three-phase MNS into a real and an imaginary part, and then setting the real part to be zero except for the pure resistance term, we eliminated the inductance effect in the real part. Then, we applied the current solution to the imaginary part and determined the capacitance value, which satisfied the imaginary part to be zero. Since the proposed method suppresses the impedance except for the resistance component of each phase, there is an advantage that can maintain the output current and the magnitude of RMF constant even if the frequency of the RMF increases. This research will allow the MNS composed of multiple electromagnets to generate the effective magnitude of the RMF with high frequency and contribute to generating fast drilling motion of the micro helical robot to tunnel through clogged lesions in blood vessels.

ACKNOWLEDGMENTS

This research was supported by a grant of the Korea Health Technology R & D Project through the Korea Health Industry Development Institute (KHIDI), funded by the Ministry of Health & Welfare, Republic of Korea (grant number: HI19C1055).

AUTHOR DECLARATIONS

Conflict of Interest

The authors have no conflicts to disclose.

Author Contributions

J. Kwon: Conceptualization (lead); Formal analysis (lead); Software (lead); Validation (equal); Writing – original draft (lead). **J. Sa:** Formal analysis (supporting); Investigation (supporting); Validation (equal); Visualization (supporting). **D. Lee:** Formal analysis (supporting); Investigation (supporting); Software (supporting); Validation (equal). **G. Jang:** Funding acquisition (lead); Project administration (lead); Supervision (lead); Writing – review & editing (lead).

DATA AVAILABILITY

The data that support the findings of this study are available from the corresponding author upon reasonable request.

REFERENCES

- ¹Q. Wang, X. Du, D. Jin, and L. Zhang, *ACS Nano* **16**, 604 (2022).
- ²J. Nam, W. Lee, B. Jang, and G. Jang, *IEEE Transactions on Industrial Electronics* **64**, 4701 (2017).
- ³K. T. Nguyen, B. Kang, E. Choi, J.-O. Park, and C.-S. Kim, *IEEE/ASME Transactions on Mechatronics* **25**, 2398 (2020).
- ⁴J. Nam, W. Lee, E. Jung, and G. Jang, *IEEE Transactions on Industrial Electronics* **65**, 5673 (2018).